J|A|C|S
A R T I C L E S

Two-Way Photoswitching Using One Type of Near-Infrared Light, Upconverting Nanoparticles, and Changing Only the Light Intensity

John-Christopher Boyer, Carl-Johan Carling, Byron D. Gates, and Neil R. Branda*

4D LABS, Department of Chemistry, Simon Fraser University, 8888 University Drive, Burnaby, British Columbia V5A 1S6, Canada

Received August 10, 2010; E-mail: nbranda@sfu.ca

Abstract: Only one type of lanthanide-doped upconverting nanoparticle (UCNP) is needed to reversibly toggle photoresponsive organic compounds between their two unique optical, electronic, and structural states by modulating merely the intensity of the 980 nm excitation light. This reversible "remote-control" photoswitching employs an excitation wavelength not directly absorbed by the organic chromophores and takes advantage of the fact that designer core−shell−shell $NaYF_4$ nanoparticles containing Er^{3+}/Yb^{3+} and Tm^{3+}/Yb^{3+} ions doped into separate layers change the type of light they emit when the power density of the near-infrared light is increased or decreased. At high power densities, the dominant emissions are ultraviolet and are appropriate to drive the ring-closing, forward reactions of dithienylethene (DTE) photoswitches. The visible light generated from the same core−shell−shell UCNPs at low power densities triggers the reverse, ring-opening reactions and regenerates the original photoisomers. The "remote-control" photoswitching using NIR light is as equally effective as the direct switching with UV and visible light, albeit the reaction rates are slower. This technology offers a highly convenient and versatile method to spatially and temporally regulate photochemical reactions using a single light source and changing either its power or its focal point.

Introduction

The direct relationship between molecular structure and function has been universally accepted by materials scientists and is part of the foundation being used to develop the next generation of optical, electronic, and mechanical materials and devices. Being able to reversibly alter molecular structure and function is equally essential if new dynamic materials are to be practical in applications from information processing to medicine. The logic is simple and based on the argument that if a molecule's structure can be reversibly modified in a controllable and predictable manner, their properties can be regulated. A convenient way to achieve this control is to incorporate functional molecules that can be toggled back and forth between different isomeric forms in response to external stimuli. These molecular switches will provide the "on−off" control needed to regulate the properties of functional materials, miniaturized components of devices, and molecule-based machines.[1,2] Because light can be easily tuned and focused, it is a particularly appealing stimulus to spatially and temporally trigger changes in the structure of molecules and function of materials containing them in a wide range of environments-of-use, from solution to solid state.[3]

Molecular switches based on the photoresponsive dithienylethene (DTE) architecture have attracted special attention for use as the control elements in molecular devices and functional materials due to the short response time, synthetic diversity, and high fatigue-resistance of the ring-closing and ring-opening photoreactions that reversibly interconvert the two isomers (Figure 1).[4−8] Two other appealing features, essential for the operation of molecular switches in many molecular devices, are the facts that the two DTE photoisomers (ring-open and ring-closed) tend not to spontaneously interconvert in the dark, and they possess distinctly different optical and electronic properties. The most visually obvious property that differs is the color of solutions, crystals, and films made from DTE derivatives, which is based on the creation of a linearly

(1) Feringa, B. L., Ed. *Molecular Switches*; Wiley-VCH: Weinheim, 2001.
(2) Balzani, V.; Credi, A.; Venturi, M. *Molecular Devices and Machines - A Journey into the Nano World*; Wiley-VCH: Weinheim, 2003.
(3) Crano, J. C., Gugielmetti, R. J., Eds. *Organic Photochromic and Thermochromic Compounds*; Plenum Press: New York, 1999.
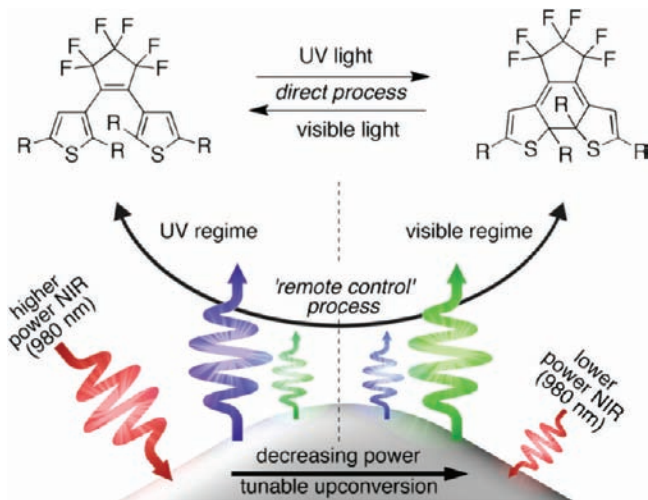(4) Irie, M. *Chem. Rev.* **2000**, *100*, 1685–1716.
(5) Tian, H.; Yang, S. *Chem. Soc. Rev.* **2004**, *33*, 85–97.
(6) Tian, H.; Wang, S. *Chem. Commun.* **2007**, 781–792.
(7) Ubaghs, L.; Sud, D.; Branda, N. R. In *Thiophene-Based Materials for Electronics and Photonics*; Perepichka, I. D., Perepichka, D., Eds.; Wiley-VCH: Germany, 2009; Vol. 2, pp 783−812.
(8) The interconversion between the two structural isomers has also been demonstrated using electricity. See: Peters, A.; Branda, N. R. *J. Am. Chem. Soc.* **2003**, *125*, 3404–3405. Peters, A.; Branda, N. R. *Chem. Commun.* **2003**, *8*, 954–955. Gorodetsky, B.; Samachetty, H.; Donkers, R. L.; Workentin, M. S.; Branda, N. R. *Angew. Chem., Int. Ed.* **2004**, *43*, 2812–2815. Gorodetsky, B.; Branda, N. R. *Adv. Funct. Mater.* **2007**, *17*, 786–796. Moriyama, Y.; Matsuda, K.; Tanifuji, N.; Irie, S.; Irie, M. *Org. Lett.* **2005**, *7*, 3315–3318. Browne, W. R.; de Jong, J. J. D.; Kudernac, T.; Walko, M.; Lucas, L. N.; Uchida, K.; van Esch, J. H.; Feringa, B. L. *Chem.-Eur. J.* **2005**, *11*, 6414–6429. Browne, W. R.; de Jong, J. J. D.; Kudernac, T.; Walko, M.; Lucas, L. N.; Uchida, K.; van Esch, J. H.; Feringa, B. L. *Chem.-Eur. J.* **2005**, *11*, 6430–6441.

Figure 1. The "direct" photoreactions of the DTE derivatives used in this study are triggered by UV light (for ring-closing) and visible light (for ring-opening). These reactions can also be triggered in a "remote control" process using the UV light generated under high excitation power densities and the visible light generated under low excitation power densities when the core−shell−shell UCNPs (**ErTm** and **TmEr**) absorb near-infrared light (980 nm). The sizes of the colored arrows represent the relative amount of each type of light excited or emitted during the multiphoton process.

π-conjugated system during ring-closing.[9,10] Other differences include how the photoisomers fluoresce or phosphoresce,[11−14] how chiral versions of them interact with plane-polarized light,[15−19] and how their magnetism[20−22] and conductivity[23−26] change. The choice of which particular property is regulated is dictated by what functional groups are attached to each end of the π-conjugated DTE backbone ("R" groups in Scheme 1). It is the tailoring of this structure−property relationship that offers molecular control in a wide range of applications including

Scheme 1. The Reversible Photoreactions Interconverting the Two DTE Isomers
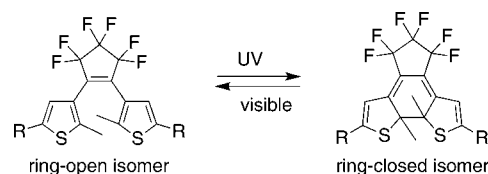
write-read-erase optical data storage,[27] information processing,[28] photorelease,[29] molecular electronics,[30] catalysis,[31−34] smart surfaces,[35] and potentially in medicine.[36,37]

A shortcoming of the DTE family is no different from one that limits the application of most photoswitches (and organic photochemistry in general) from practical use and is based on the fact that high-energy UV and visible light sources are required to trigger the photoreactions. This need for high-energy light can complicate the use of these versatile molecular systems in many applications where these wavelengths have detrimental effects. One example is their use in biological settings where UV light leads to low tissue penetration as well as mutagenesis of cells. Storing optical information in three-dimensional digital media will also suffer from similar issues, and the absorption of light by the matrix can lead to distortion of the information and shortening of storage lifetime. Unless a method to deliver lower energy light deep into tissue or solid-state materials is developed, photoswitching and organic photochemistry will have restricted appeal.

A possible solution to this problem is to use multiphoton near-infrared (NIR) light excitation to trigger the photochemical reactions. Because two-photon excitation (TPE) requires high excitation power densities, molecular systems susceptible to TPE offer the possibility to spatially address organic materials in all three dimensions. Unfortunately, the low two-photon-absorbing cross sections typical for DTE photoswitches (and other classes of photoresponsive compounds) is a significant drawback in practical applications where the use of high-intensity lasers is not feasible. This reliance on high power densities is even more of an issue in photoswitching applications because the ring-closing reaction of DTEs requires three-photon NIR excitation to generate the necessary UV or blue light, leading to even lower efficiencies. A better alternative is to introduce a photostable, sensitizing system that can absorb NIR light and convert it through a more efficient process into the UV and visible light needed to trigger the photoreactions of the DTE molecular

(9) Irie, M.; Sakemura, K.; Okinaka, M.; Uchida, K. *J. Org. Chem.* **1995**, *60*, 8305–8309.

(10) Nakayama, Y.; Hayashi, K.; Irie, M. *Bull. Chem. Soc. Jpn.* **1991**, *64*, 789–795.

(11) Nakagawa, T.; Hasegawa, Y.; Kawai, T. *J. Phys. Chem. A* **2008**, *112*, 5096–5103.

(12) Fernandez-Acebes, A.; Lehn, J.-M. *Chem.-Eur. J.* **1999**, *5*, 3285–3292.

(13) Murguly, E.; Norsten, T.; Branda, N. R. *Angew. Chem., Int. Ed.* **2001**, *40*, 1752–1755.

(14) Zhao, H.; Al-Atar, U.; Pace, T.; Bohne, C.; Branda, N. R. *J. Photochem. Photobiol.* **2008**, *200*, 74–82.

(15) Yamaguchi, T.; Uchida, K.; Irie, M. *J. Am. Chem. Soc.* **1997**, *119*, 6066–6071.

(16) Kodani, T.; Matsuda, K.; Yamada, T.; Kobatake, S.; Irie, M. *J. Am. Chem. Soc.* **2000**, *122*, 9631–9637.

(17) Yamamoto, S.; Matsuda, K.; Irie, M. *Org. Lett.* **2003**, *5*, 1769–1772.

(18) Matsuda, K.; Yamamoto, S.; Irie, M. *Tetrahedron Lett.* **2001**, *42*, 7291–7293.

(19) Yamaguchi, T.; Nomiyama, K.; Isayama, M.; Irie, M. *Adv. Mater.* **2004**, *16*, 643–645.

(20) Matsuda, K.; Irie, M. *Polyhedron* **2005**, *24*, 2477–2483.

(21) Tanifuji, N.; Irie, M.; Matsuda, K. *J. Am. Chem. Soc.* **2005**, *127*, 13344–13353.

(22) Sun, L.; Tian, H. *Tetrahedron Lett.* **2006**, *47*, 9227–9231.

(23) Dulic, D.; van der Molen, S. J.; Kudernac, T.; Jonkman, H. T.; de Jong, J. J. D.; Bowden, T. N.; van Esch, J.; Feringa, B. L.; van Wees, B. J. *Phys. Rev. Lett.* **2003**, *91*, 207402.

(24) Matsuda, K.; Yamaguchi, H.; Sakano, T.; Ikeda, M.; Tanifuji, N.; Irie, M. *J. Phys. Chem. C* **2008**, *112*, 17005–17010.

(25) Kronemeijer, A. J.; Akkerman, H. B.; Kudernac, T.; van Wees, B. J.; Feringa, B. L.; Blom, P. W. M.; de Boer, B. *Adv. Mater.* **2008**, *20*, 1467–1473.

(26) Whalley, A. C.; Steigerwald, M. L.; Guo, X.; Nuckolls, C. *J. Am. Chem. Soc.* **2007**, *129*, 12590–12591.

(27) Myles, A. J.; Branda, N. R. *Adv. Funct. Mater.* **2002**, *12*, 167–173.

(28) Andreasson, J.; Straight, S. D.; Moore, T. A.; Moore, A. L.; Gust, D. *J. Am. Chem. Soc.* **2008**, *130*, 11122–11128.

(29) Lemieux, V.; Gauthier, S.; Branda, N. R. *Angew. Chem., Int. Ed.* **2006**, *45*, 6820–6824.

(30) Belser, P.; De Cola, L.; Hartl, F.; Adamo, V.; Bozic, B.; Chriqui, Y.; Iyer, V. M.; Jukes, R. T. F.; Kuhni, J.; Querol, M.; Roma, S.; Salluce, N. *Adv. Funct. Mater.* **2006**, *16*, 195–208.

(31) Vomasta, D.; Högner, C.; Branda, N. R.; König, B. *Angew. Chem., Int. Ed.* **2008**, *47*, 7644–7647.

(32) Samachetty, H. D.; Lemieux, V.; Branda, N. R. *Tetrahedron* **2008**, *64*, 8292–8300.

(33) Lemieux, V.; Spantulescu, M. D.; Baldridge, K. K.; Branda, N. R. *Angew. Chem., Int. Ed.* **2008**, *120*, 5112–5115.

(34) Samachetty, H. D.; Branda, N. R. *Pure Appl. Chem.* **2006**, *78*, 2351–2359.

(35) Browne, W. R.; Kudernac, T.; Katsonis, N.; Areephong, J.; Feringa, B. L. *J. Phys. Chem. C* **2008**, *112*, 1183–1190.

(36) Al-Atar, U.; Fernandes, R.; Johnsen, B.; Baillie, D.; Branda, N. R. *J. Am. Chem. Soc.* **2009**, *131*, 15966–15967.

(37) Sud, D.; Wigglesworth, T. J.; Branda, N. R. *Angew. Chem., Int. Ed.* **2007**, *46*, 8017–8019.

switch in a "remote control" process. Lanthanide-doped upconverting nanoparticles (UCNPs)[38−44] are ideal sensitizers for this task and are the systems described in this Article.

UCNPs convert low energy NIR light into higher energy UV and visible light through several unique mechanisms.[45] The lower excitation power density requirements of UCNPs versus traditional TPE fluorophores such as dyes and quantum dots arise from the fact that the intermediate levels involved in the upconversion mechanisms are real metastable energy levels. The most efficient UCNPs known to date are hexagonal β-phase $NaYF_4$ nanoparticles doped with either the Er/Yb or the Tm/Yb ion couples.[46] Violet, green, and red emissions are generated from the Er/Yb-doped UCNPs, while UV, blue, and NIR emissions have been observed in the case of the Tm/Yb-doped analogues. The high efficiency of the upconversion processes in hexagonal $NaYF_4$ nanoparticles can be attributed a combination of two factors: (1) the low-energy phonons of the $NaYF_4$ hexagonal matrix, which minimizes nonradiative relaxation of the excited states, and (2) the interatom spacing between the dopant ions, which increases the efficacy of the energy transfer processes. The majority of the studies in the literature have focused on the visible emissions from these UCNPs with only a few reporting on the UV upconversion emissions that are capable of being generated from Tm^{3+}/Yb^{3+}-doped materials. Yet, these UV emissions are critical to develop a "universal" method to drive photochemical reactions, especially those necessary in applications where UV radiation cannot be used such as in biological tissues and fluids.[47,48]

Lanthanide-doped upconverting nanoparticles have many other favorable characteristics that explain the recent interest generated by them including resistance to photodegradation, lack of blinking, and the ability to be excited with compact and relatively inexpensive NIR diode lasers.[49] The bulk of the reported studies on UCNPs are aimed at advancing the synthetic methods for the production of these materials[38−44] as well as postsynthetic surface treatments to enable their use in bioimaging and biomedicine for cell imaging, disease detection, and treatment.[50] Other possible explored uses for UCNPs range from artificial lighting and sensitized solar-cells[51] to security labeling.[52] What has not been as well demonstrated is how these nanoparticles can be used to drive important photochemical reactions.

We recently demonstrated how we could trigger DTE photoswitches to undergo both their ring-closing and their ring-opening reactions using the same wavelength of NIR light (980 nm) and two different lanthanide-doped UCNPs.[53] The photoswitches do not absorb this NIR wavelength directly, and the photoreactions (including one that has an accompanying thermal release of a small molecule) are induced by the blue light generated from Tm^{3+}/Yb^{3+}-doped (for ring-closing) and the green light generated from Er^{3+}/Yb^{3+}-doped (for ring-opening) $NaYF_4$ nanoparticles. Before our recent report, the few studies that combine dithienylethenes and lanthanide-doped upconverting nanoparticles focused on nondestructive optical memory, where the ring-closed isomer of the DTE photoswitch selectively quenches the luminescence from the UCNP through an energy transfer process, providing a read-out signal in the NIR.[54,55] However, UV light (for writing) and visible light (for erasing) are still required as these steps are a result of the ring-closing and ring-opening reactions of the photoswitch, respectively. NIR-induced photoswitching in these studies was not observed using 980 nm irradiation due to the low efficiencies of the UCNPs and the low excitation densities used.

What may limit the use of our first-generation multiphoton systems is the fact that only one of the photoreactions can be selected by choosing the appropriate lanthanide dopant (Tm^{3+} or Er^{3+}). We now demonstrate how we can use only one type of layered, hybrid core−shell−shell nanoparticle and a single wavelength of NIR light to toggle examples of this important class of photoswitches between their two isomers. We illustrate that the direction of the chromophore's photoreaction can be controlled by increasing (for ring-closing) or decreasing (for ring-opening) the power density of the laser, which controls the color of the light emitted from our designer nanoparticles.

The concept is summarized in Figure 1 and is based on the documented fact that the intensities of the upconversion emissions from lanthanide-doped materials are highly dependent on the power density of the excitation source.[56] The green and red emissions from the Er/Yb-doped UCNPs have a quadratic dependence on the excitation source, while the UV and blue emissions in Tm/Yb-doped UCNPs require 4 and 5 photons to induce them. The implication is that at much higher power densities, UV luminescence will be generated from Tm/Yb, while green and red emissions can be generated from Er/Yb UCNPs at lower power densities. The green and red upconversion mechanisms will also saturate and plateau at lower power densities than the UV emissions. The consequence of this phenomenon is that core−shell−shell UCNPs synthesized to contain different lanthanide ions in different layers will produce a single nanoparticle system capable of inducing both ring-closing and ring-opening reactions of DTE derivatives. By placing the lanthanides in separate layers, the quenching of the upconversion luminescence by cross-relaxation between the various dopant ions is minimized. This Article represents a relatively universal example of how multiphoton processes in nanoparticles can be used to induce important photoreactions

(38) Heer, S.; Kompe, K.; Güdel, H. U.; Haase, M. *Adv. Mater.* **2004**, *16*, 2102–2105.

(39) Mai, H. X.; Zhang, Y. W.; Si, R.; Yan, Z. G.; Sun, L. D.; You, L. P.; Yan, C. H. *J. Am. Chem. Soc.* **2006**, *128*, 6426–6436.

(40) Boyer, J. C.; Vetrone, F.; Cuccia, L. A.; Capobianco, J. A. *J. Am. Chem. Soc.* **2006**, *128*, 7444–7445.

(41) Boyer, J. C.; Cuccia, L. A.; Capobianco, J. A. *Nano Lett.* **2007**, *7*, 847–852.

(42) Mai, H. X.; Zhang, Y. W.; Sun, L. D.; Yan, C. H. *J. Phys. Chem. C* **2007**, *111*, 13730–13739.

(43) Li, Z. Q.; Zhang, Y. *Nanotechnology* **2008**, *19*, 345606.

(44) Li, Z. Q.; Zhang, Y.; Jiang, S. *Adv. Mater.* **2008**, *20*, 4765–4769.

(45) Scheps, R. *Prog. Quantum Electron.* **1996**, *20*, 271–358.

(46) Krämer, K. W.; Biner, D.; Frei, G.; Güdel, H. U.; Hehlen, M. P.; Lüthi, S. R. *Chem. Mater.* **2004**, *16*, 1244–1251.

(47) Goeldner, M.; Givens, R. *Dynamic Studies in Biology*; Wiley-VCH Verlag GmbH & Co. KGaA: Weinheim, 2005.

(48) Adams, S. R.; Tsien, R. Y. *Annu. Rev. Physiol.* **1993**, *55*, 755–784.

(49) Wu, S.; Han, G.; Milliron, D. J.; Aloni, S.; Altoe, V.; Talapin, D. V.; Cohen, B. E.; Schuck, P. J. *Proc. Natl. Acad. Sci. U.S.A.* **2009**, *106*, 10917–10921.

(50) Boyer, J. C.; Manseau, M. P.; Murray, J. I.; van Veggel, F. C. J. M. *Langmuir* **2010**, *26*, 1157–1164.

(51) Shalav, A.; Richards, B. S.; Trupke, T.; Kramer, K. W.; Gudel, H. U. *Appl. Phys. Lett.* **2005**, *86*, 013505.

(52) Kim, W. J.; Nyk, M.; Prasad, P. N. *Nanotechnology* **2009**, *20*, 185301.

(53) Carling, C.-J.; Boyer, J.-C.; Branda, N. R. *J. Am. Chem. Soc.* **2009**, *131*, 10838–10839.

(54) Zhou, Z.; Yang, H.; Tao, Y.; Huang, K.; Yu, M.; Li, F.; Huang, C. *Chem. Commun.* **2008**, *39*, 4786–4788.

(55) Zhang, C.; Zhou, H. P.; Liao, L.-Y.; Feng, W.; Sun, W.; Li, Z.-X.; Xu, C.-H.; Fang, C.-J.; Sun, L.-D.; Zhang, Y. W.; Yan, C.-H. *Adv. Mater.* **2009**, *22*, 633–637.

(56) Boyer, J. C.; Johnson, N. J. J.; van Veggel, F. C. J. M. *Chem. Mater.* **2009**, *21*, 2010–2012.

of organic chromophores even when they require high-energy, differing wavelengths of light.

Results and Discussion

Choice and Synthesis of DTEs and Nanoparticles. Photoresponsive DTE derivatives **1** and **2** were chosen to demonstrate the concepts described in the introduction of this Article and were synthesized using methods previously described by our group.[57,58] The DTE backbone has been tailored to optimize the efficacy of the "remote control" processes to avoid the need for a polymer matrix to maintain the close proximity of the photoswitch and UCNPs as was the case in our original report.
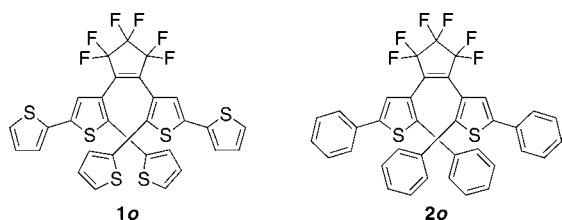
All studies described in this Article use colloidal solutions of the photoresponsive compounds and the UCNPs. We continued to employ core−shell hexagonal $NaYF_4$ nanoparticles synthesized in high boiling point solvents because these UCNPs have been consistently shown to be the most efficient upconverters known to date. We used a modified method of a literature synthesis procedure to synthesize all the core−shell and core−shell−shell UCNPs used in these studies.[59] Four different lanthanide-doped $NaYF_4$ nanoparticles were used to demonstrate reversible, power-regulated photoswitching with a single set of UCNPs and determine which lanthanide should be doped in which layer of the core−shell−shell nanoparticles. Two of them (referred to as **Er** and **Tm**) have the lanthanides (Er^{3+} and Tm^{3+}) doped only in their core and are surrounded by a shell of $NaYF_4$ to minimize quenching of the emission due to solvent interactions. The other two (**ErTm** and **TmEr**) have two shells wrapped around a core of lanthanide-doped $NaYF_4$. The first (**ErTm**) has $NaYF_4$, 2 mol % Er^{3+}, 20 mol % Yb^{3+} as the core material, $NaYF_4$, 0.5 mol % Tm^{3+}, 30 mol % Yb^{3+} as the first shell and $NaYF_4$ as the outermost shell. The second (**TmEr**) has the two lanthanide-doped layers reversed. In this case, the core is made up of $NaYF_4$, 0.5 mol % Tm^{3+}, 30 mol % Yb^{3+}, covered in a shell of $NaYF_4$, 2 mol % Er^{3+}, 20 mol % Yb^{3+}. The outermost shell remains $NaYF_4$. The composition of each nanoparticle is listed in Table 1.

All UCNPs were prepared using a three-step synthetic method in which lanthanide-doped core nanoparticles were successively coated with a lanthanide-doped first shell followed by an undoped $NaYF_4$ final shell. This core−shell method has been previously shown to allow for more efficient upconversion from Er^{3+} and Tm^{3+} than doping the two ions into a single UCNP.[59] For the **ErTm** sample, $NaYF_4$, 2 mol % Er^{3+}, 20 mol % Yb^{3+} nanoparticles were utilized as seeds to grow a $NaYF_4$, 0.5 mol % Tm^{3+}, 30 mol % Yb^{3+} shell. This was subsequently followed by the growth of an undoped $NaYF_4$ shell to further increase the efficiency of the upconversion processes as has been effectively established by several research groups.[50,59] In a fashion similar to that for the **TmEr** sample, $NaYF_4$, 0.5 mol

(57) Peters, A.; Branda, N. R. *J. Am. Chem. Soc.* **2003**, *125*, 3404–3405.
(58) Peters, A.; McDonald, R.; Branda, N. R. *Chem. Commun.* **2002**, 2274–2275.
(59) Qian, H. S.; Zhang, Y. *Langmuir* **2008**, *21*, 12123–12125.

Table 1. Constituent Lanthanide Dopants in Each Layer of All Upconverting Nanoparticles Used in These Experiments[a]

UCNP	core		inner shell	
	mol % dopant	volume (nm³)	mol % dopant	volume (nm³)
Er	2.0 Er^{3+} 20 Yb^{3+}	31 660	none	
Tm	0.5 Tm^{3+} 30 Yb^3	114 965	none	
ErTm	2.0 Er^3 20 Yb^{3+}	39 300	0.5 Tm^{3+} 30 Yb^{3+}	40 605
TmEr	0.5 Tm^{3+} 30 Yb^{3+}	57 800	2.0 Er^{3+} 20 Yb^{3+}	51 040

[a] In all cases, the nanoparticle matrix is $NaYF_4$.

% Tm^{3+}, 30 mol % Yb^{3+} cores were coated with a $NaYF_4$, 2 mol % Er^{3+}, 20 mol % Yb^{3+} followed by an undoped $NaYF_4$ shell. The architectures of the two types of core−shell−shell UCNPs are illustrated in Figure 2.

All the synthesized nanoparticles were successfully indexed to hexagonal-phase $NaYF_4$ (JCPDS standard card 16-0334) according to powder X-ray diffraction (Figure S1). Transmission electron microscopy (TEM) images of the UCNPs (Figures 2 and S2−S5) show that they are all single crystalline in nature, possess uniform ellipsoid shapes, and have nearly monodisperse particle sizes (with average diameters of 35.7 and 38.8 nm for the **ErTm** and **TmEr** samples, respectively). As observed in the TEM images of the **ErTm** and **TmEr** UCNPs (Figure 2), each successive shell formation resulted in an increase of the average diameter of the nanoparticles, indicating successful shell growth. This procedure results in discrete shells with a minimal amount of alloying at the interface between each of them. The separation of the dopants into two different layers of the nanoparticles is important to maximize the efficiency of the upconversion processes as doping all of the lanthanide ions in one layer would lead to nonradiative energy transfers and lower upconversion efficiencies. For each core−shell−shell UCNP, the volumes of the core and first shell containing the lanthanide dopants are similar to each other (Table 1). This similarity is important because the ratio of dopants in each nanoparticle must be the same to rule out any changes in the multiphoton processes between nanoparticles due to a difference in the amount of lanthanide responsible for the process. The differences in emission and photoswitching that will be discussed later in this Article are, therefore, due to where each lanthanide ion is located in the nanoparticle and not its amount.

Optical Properties of UCNPs. The upconversion luminescence spectra (λ_{ex} = 980 nm) of the **Er** and **Tm** core−shell UCNPs dispersed as 1.5 wt % colloids in THF are shown in Figure 3c and d. These spectra were acquired using similar power densities that will eventually be employed to mediate the photoreactions of the photoswitches (500 W/cm² for ring-closing with **Tm** and 15 W/cm² for ring-opening with **Er**). For the **Tm** nanoparticles, upconversion emission peaks at 290, 350, 365, 450, and 475 nm were observed corresponding to the $^3P_0 \rightarrow {}^3H_6$, $^3P_0 \rightarrow {}^3F_4$, $^1D_2 \rightarrow {}^3H_6$ $^1D_2 \rightarrow {}^3F_4$, and $^1G_4 \rightarrow {}^3H_6$ transitions. Emissions from 630 to 750 nm were also observed and attributed to the $^1G_4 \rightarrow {}^3F_4$ and $^3F_3 \rightarrow {}^3H_6$ transitions. The particular peaks of interest for ring-closing **1o** and **2o** are those in the UV/blue regions of the spectrum (290, 350−365 nm) as these are the ones that have appropriate spectral overlap with the high-energy absorption bands (300−350 nm) of THF solutions of the ring-open forms of the two photoswitches (Figure 3a and b).

For solutions of the **Er** UCNPs, emissions centered at 409, 520, 541, and 653 nm were observed and assigned to the $^4H_{9/2}$
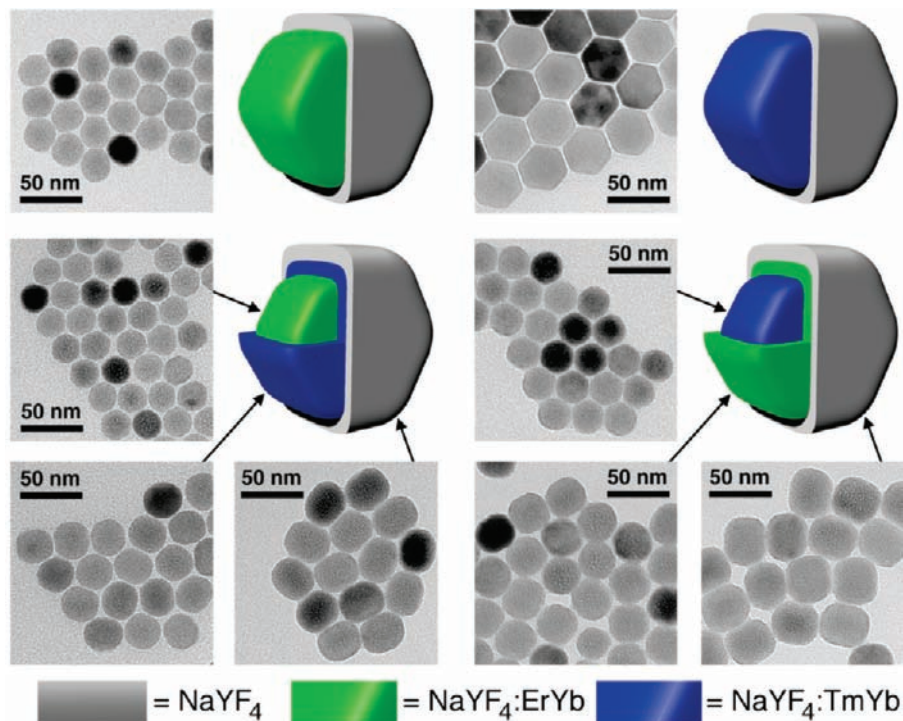
Figure 2. TEM images of the core, core−shell, and core−shell−shell nanoparticles for NaYF$_4$:ErYb-NaYF$_4$ (**Er**), NaYF$_4$:TmYb-NaYF$_4$ (**Tm**), NaYF$_4$:ErYb-NaYF$_4$:TmYb-NaYF$_4$ (**ErTm**), and NaYF$_4$:TmYb-NaYF$_4$:ErYb-NaYF$_4$ (**TmEr**) UCNPs illustrating their uniform size and shape.

$\rightarrow$ $^4I_{15/2}$, $^4H_{11/2} \rightarrow {}^4I_{15/2}$, $^5S_{3/2} \rightarrow {}^4I_{15/2}$, and $^4F_{9/2} \rightarrow {}^4I_{15/2}$ transitions, respectively. In this case, it is the green (520−550 nm) and the red (640−670 nm) upconversion emissions that have suitable spectral overlap with the absorption bands corresponding to the ring-closed forms of both photoswitches. These emissions will be utilized to trigger the ring-opening photoreactions of the photoswitches (**1c** → **1o** and **2c** → **2o**).

Figure 3e and f shows the upconversion luminescence spectra of the **ErTm** and **TmEr** core−shell−shell UCNPs at high (500 W/cm^2) and low (15 W/cm^2) power densities and highlights the changes in the intensities of the emissions. In the high power excitation regime, all of the expected Tm^{3+} and Er^{3+} upconversion emissions are present in the spectra for both **ErTm** and **TmEr** UCNPs, although there are significant differences in the relative intensities of the emissions. As postulated in the Introduction, the intensities of the emission peaks due to Tm^{3+} are all much larger than those for the Er^{3+} emissions in both nanoparticles. The major difference between the two nanoparticles at high irradiation power is that the dominance of the Tm^{3+} emissions is even greater in the case of the **TmEr** UCNPs, demonstrating that placing the Tm^{3+} ions in the core of the nanoparticles maximizes the UV and blue emissions as compared to when this lanthanide is doped into the first shell. This is not due to a difference in the amount of Tm^{3+} ions in the core as compared to the first shell because the volume of each is virtually the same (Table 1).

On the other hand, the emissions from Er^{3+} ions dominate in both types of core−shell−shell nanoparticle (**ErTm** and **TmEr**) at lower power density (15 W/cm^2), and only trace contributions in the UV and blue regions due to the Tm^{3+} dopant are observable. The results summarized in Figure 3 support the hypothesis that by varying only the excitation laser power density and not the wavelength of the excitation beam, the emissive properties of the UCNPs and, thus, the direction of DTE photoswitching can be controlled. Both types of core−shell−

shell nanoparticle are stable under even the high-power irradiation conditions, and no changes in their emission spectra are observed after 1 h exposure (Figure S7).

"Remote Control" Photoswitching of DTE Derivatives. To determine what is the maximum efficiency for the "remote control" photoreactions of DTE compounds **1** and **2**, the core−shell UCNPs were first examined for their ability to drive the ring-closing reactions (using **Tm**) and the ring-opening reactions (using **Er**). The ability of the UV emissions generated by Tm^{3+} dopant to trigger the photocyclization reactions was assessed by irradiating solutions of **1o** and **2o** (1.5×10^{-5} M) containing **Tm** nanoparticles (1.5 wt %) with a 980 nm laser (power density of 500 mW/cm^3). The colors of the solutions changed from colorless to a blue or blue/green, which can be attributed to the photocyclization reactions **1o** → **1c** and **2o** → **2c**, respectively. The success of these reactions is supported by the changes in the absorption spectra of the photoswitches, which match those for **1o** and **2o** when they are irradiated with UV light as shown in the Supporting Information. Both photoswitches reached similar photostationary states when irradiated with NIR light and the nanoparticle ("remote control" process) as with a hand-held 313 nm mercury lamp ("direct" process; horizontal line in Figure 4a), effectively demonstrating that the intensity of the UV upconversion emissions from the **Tm** UCNPs is enough to effectively drive the reaction to completion (or at least as complete as possible).

In a similar fashion, the green and red upconversion emissions from the **Er** UCNPs can equally be employed to drive the ring-opening reactions of the two photoswitches. This is demonstrated by irradiating THF solutions containing **1c** or **2c** (generated with 313 nm light) and **Er** UCNPs with 980 nm laser light (15 W/cm^2), which results in the complete decolorizing of the solutions and regeneration of the absorption spectra corresponding to the ring-open isomers (**1o** and **2o**). The "remote control" ring-opening reactions (**1c** → **1o** and **2c** → **2o**) are supported
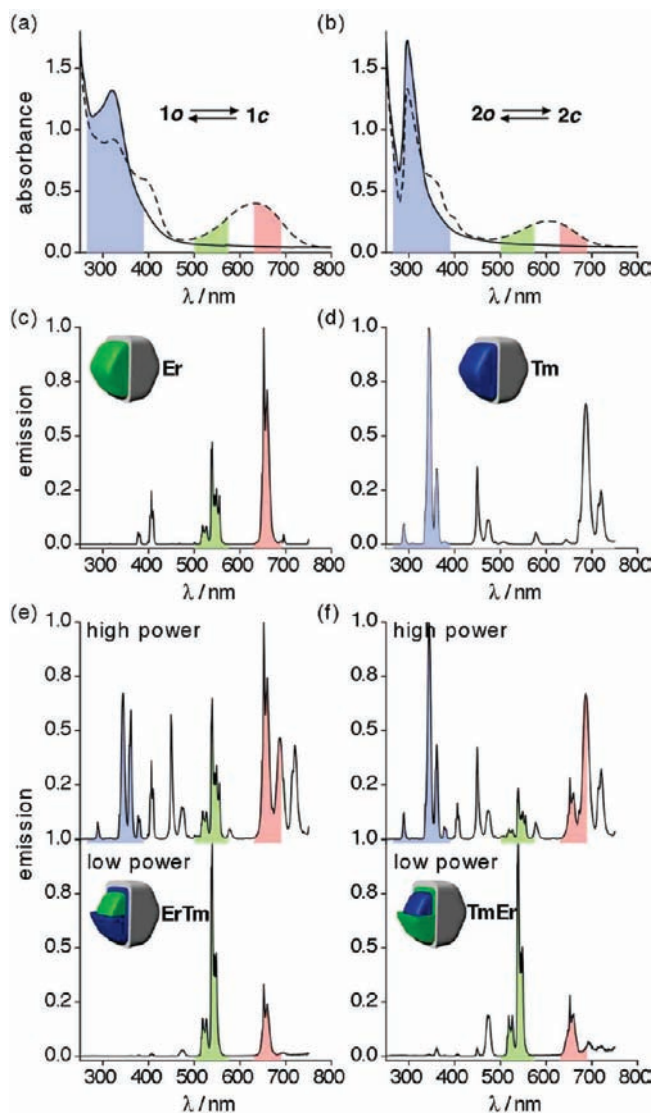
Figure 3. UV−vis absorption spectra of THF solutions (1.5×10^{-5} M) of (a) **1o** and (b) **2o** before (solid line) and after irradiation with 365 nm light (dashed line) for 2 min. Emission spectra of THF solutions (1.5 wt %, λ_{ex} = 980 nm) of (c) NaYF$_4$:ErYb (**Er**) and (d) NaYF$_4$:TmYb (**Tm**) core−shell UCNPs, and of (e) **ErTm** and (f) **TmEr** core−shell−shell UCNPs at high power (500 W/cm^2, top graph) and low power (15 W/cm^2, bottom graph). The shaded, colored regions in all cases represent each emission region and show the suitable spectral overlap with the appropriate absorption bands for the ring-open and ring-closed isomers of DTEs **1** and **2**.

by spectral changes that match those for samples of **1c** and **2c** when they are irradiated with visible light (wavelengths greater than 450 nm). Once again, both reactions can be driven close to completion using the **Er** UCNPs (Figure 4b). The fact that the photoreactions of either DTE photoswitch are driven by absorbing the light generated by the UCNPs is demonstrated by irradiating solutions of each DTE with 980 nm laser light but without any of the nanoparticles, which undergo no visible changes in their colors or UV−vis spectra.

The reversible photoswitching of both dithienylethene photoswitches with a single set of UCNPs was demonstrated using combinations of the **ErTm** and **TmEr** nanoparticles with the two photoswitches (**1** and **2**). The ability of each UCNP to induce the ring-opening and ring-closing photoreactions of the DTEs was examined by comparing how quickly and to what extent the **ErTm** and **TmEr** UCNPs could drive the reactions
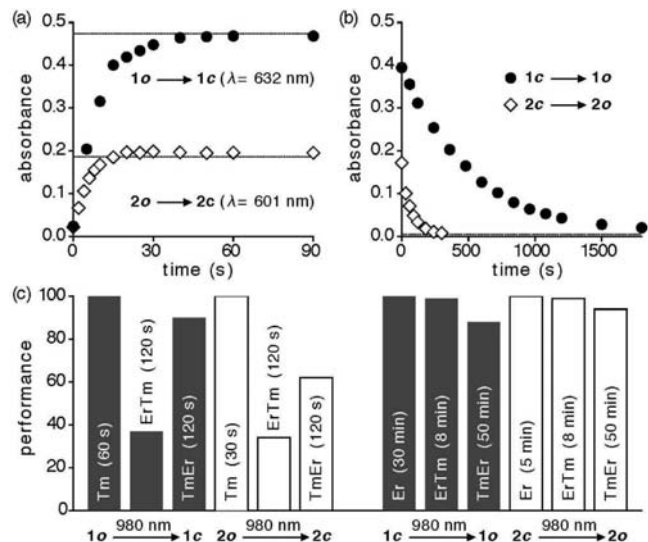

Figure 4. Changes in the absorbances (λ_{max} = 632 and 601 nm for **1c** and **2c**, respectively) when THF solutions of (a) DTEs **1o** and **2o** containing NaYF$_4$:TmYb nanoparticles (**Tm**) are irradiated with 980 nm light at high excitation power densities (500 W/cm^2), and (b) DTEs **1c** and **2c** containing NaYF$_4$:ErYb (**Er**) nanoparticles are irradiated with 980 nm light at low excitation power densities (15 W/cm^2). The horizontal lines show the absorbance values when similar solutions are irradiated with UV light (313 nm) for graph a or visible light (>450 nm) for graph b until the photostationary states are obtained. (c) The degree to which the ring-closing and ring-opening reactions are induced with 980 nm light (high power for the former and low power for the latter) using the different types of nanoparticles.

as compared to the **Er** and **Tm** core−shell nanoparticles, which were optimized for this task. We call this efficiency "performance", which is plotted in Figure 4c for all DTE/nanoparticle combinations as a percent. The extent of the "remote control" photoswitching induced by **Er** and **Tm** was set as 100%.

For compound **1**, the best performance was achieved with the **TmEr** UCNPs, which drove the ring-closing photoreaction (**1o** → **1c**) to within 90% of the photostationary state obtained with the **Tm** UCNPs, albeit in twice the length of time (120 s). When the **ErTm** nanoparticles are used, the photostationary state is reached after the same irradiation time; however, the amount of ring-closed isomer in this photostationary state is less than one-half (37%) of what is was with the **TmEr** nanoparticles. The same is true for compound **2o**, although the photostationary states generated using both types of core−shell−shell UCNP are slightly lower than for DTE **1o** (62% when **TmEr** is used and 34% when **ErTm** is used). These observations make sense because the nanoparticles that have the Tm^{3+} ions in the core generate substantially more UV and blue light than when the ion resides in the first shell (compare the spectra in Figure 3e and f). The lower photostationary states for **2o** → **2c** as compared to **1o** → **1c** are a reflection of the intrinsic photoswitching behavior of these DTE derivatives, where the former is only 42% when **1o** exposed to direct UV light (313−365 nm), while the latter is 80%.[57,58]

Because both core−shell−shell UCNPs generate similar emissions at low power (Figure 3e and f), they should be almost equally effective at driving the ring-opening reactions of the photochromic DTEs. Figure 4c shows this to be the case. The **1c** → **1o** photoreaction was driving back to within 88% of the level obtained employing the **Er** UCNPs when **TmEr** is used and nearly driven to completion (99%) when **ErTm** is used in a shorter period of time. This allows for a choice in
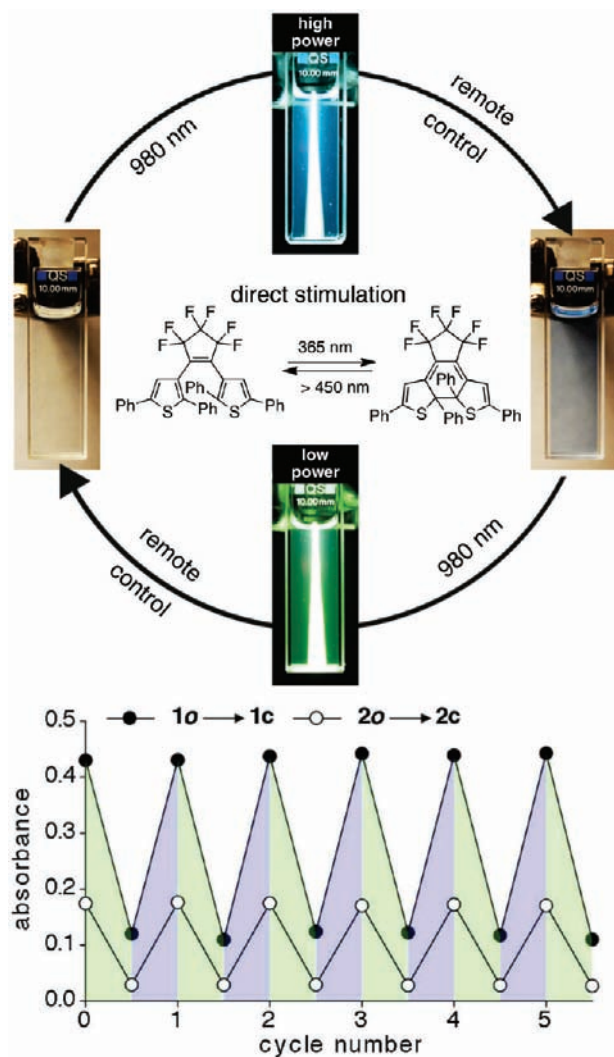
Figure 5. Bidirectional photoswitching of a THF solution of DTE **2** dispersed with **TmEr** core−shell−shell nanoparticles by varying only the intensity of the NIR light. The plot shows the absorption intensities corresponding to the ring-closed isomers (632 nm for **1c** and 601 nm for **2c**) as solutions of the photoswitches and the core−shell−shell nanoparticles are exposed to alternating intensities of 980 light. The colors correspond to the light emitted by the nanoparticles (green at low power and blue at high power).

performance between the two sets of core−shell−shell UCNPs. Both the **ErTm** and the **TmEr** UCNPs were capable of driving the **2o → 2c** photoreaction to within 99% and 94% of the level obtained with the **Er** nanoparticles. Faster kinetics for the ring-opening reaction is again obtained with the **ErTm** sample (8 min) than with the **TmEr** sample (50 min) due to the decreased amount of UV emissions at low excitation powers.

Figure 5 shows a visual representation of the bidirectional photoswitching for DTE **2** and the **TmEr** nanoparticles by simply using the power of the 980 nm excitation beam as the control mechanism. The two solutions, colorless and blue, can be interconverted by irradiating them with 980 nm light and dialing in the power, "high" to produce the blue and UV light needed to trigger ring-closing (**2o → 2c**) or "low" to produce the green light to regenerate the original color due to ring-opening (**2c → 2o**). Figure 5 also shows the absorption intensities at 632 nm for **1** and 601 nm for **2** as solutions of them are cycled between ring-closed and ring-open forms when exposed to varying intensity 980 nm light sources, illustrating the reversibility of the system.

Conclusion

In this Article, we have demonstrated how we can employ lanthanide-doped core−shell−shell upconverting nanoparticles to reversibly toggle a pair of dithienylethene photoresponsive molecules in a "remote-control" fashion using a single wavelength of near-infrared light (980 nm) and by adjusting only the excitation power. This was achieved by preferentially doping the Er^{3+} and Tm^{3+} emissive ions into separate layers of the UCNPs, resulting in the more efficient upconversion processes required to drive the reversible photoswitching reactions. The key aspect was the nonlinearity of the upconversion mechanisms, which results in the selective generation of UV and blue light under high-power conditions, which triggers ring-closing of the DTEs. Conversely, the reverse, ring-opening reactions can be triggered by simply reducing the power density of the excitation light to the point where the visible Er^{3+} upconversion emissions dominate. Through the combination of core−shell−shell UCNPs and DTE photoswitches, we have created the first photochromic system that can be modulated simply with the power of the excitation light.

Improvements to the system are still possible. Attaching the photoswitches to the surface of the nanoparticles will increase the amount of energy transfer between the components and decrease the amount of irradiation time required for the photoreactions to occur. In addition, improvements to the upconversion properties of the various UCNPs are still possible and must be examined in greater detail to optimize the amount of each type of emission under various power densities.

Supporting Information Available: Experimental procedures and XRD, TEM, and UV−vis absorption spectroscopy characterizations. This material is available free of charge via the Internet at http://pubs.acs.org.

JA107184Z